Evaluation of an intramedullary bone stabilization system using a light-curable monomer in sheep

Citation: Zani, Brett G., Rose Baird, James R. L. Stanley, Peter M. Markham, Markus Wilke, Stephan Zeiter, Aswin Beck, et al. "Evaluation of an Intramedullary Bone Stabilization System Using a Light-Curable Monomer in Sheep." J. Biomed. Mater. Res. 104, no. 2 (March 12, 2015): 291–299.

As Published: http://dx.doi.org/10.1002/jbm.b.33380

Publisher: Wiley Blackwell

Persistent URL: http://hdl.handle.net/1721.1/102787

Version: Author's final manuscript: final author's manuscript post peer review, without publisher's formatting or copy editing

HHS Public Access

Author manuscript

J Biomed Mater Res B Appl Biomater. Author manuscript; available in PMC 2016 February 01.

Published in final edited form as:

J Biomed Mater Res B Appl Biomater. 2016 February ; 104(2): 291–299. doi:10.1002/jbm.b.33380.

Evaluation of an Intramedullary Bone Stabilization System Using a Light-Curable Monomer in Sheep

Brett G. Zani[1], **Rose Baird**[1], **James R.L. Stanley**[1], **Peter M. Markham**[1], **Markus Wilke**[2], **Stephan Zeiter**[2], **Aswin Beck**[2], **Dirk Nehrbass**[2], **Gregory A. Kopia**[3], **Elazer R. Edelman**[4], and **Robert Rabiner**[5]

[1]CBSET, Inc. 500 Shire Way, Lexington, MA 02421 [2]AO Foundation, Clavadelerstrasse 8, 7270 Davos, Switzerland [3]Kopia Consulting, 61-4D Taurus Drive, Hillsborough, NJ 08844 [4]Institute for Medical and Engineering Science, Massachusetts Institute of Technology E25, 45 Carleton St., Cambridge, MA, 02139 [5]IlluminOss Medical Inc. 993 Waterman Ave., East Providence, RI 02914

Abstract

Percutaneous intramedullary fixation may provide an ideal method for stabilization of bone fractures, while avoiding the need for large tissue dissections. Tibiae in 18 sheep were treated with an intramedullary photodynamic bone stabilization system (PBSS) comprised of a polyethylene terephthalate (Dacron) balloon filled with a monomer and cured with visible light *in situ* then harvested at 30, 90 or 180 days. In an additional 40 sheep, a mid-shaft tibial osteotomy was performed and stabilized with external fixators or external fixators combined with the PBSS and evaluated at 8, 12 and 26 weeks. Healing and biocompatibility were evaluated by radiographic analysis, microCT and/or histopathology. In non-fractured sheep tibiae, PBSS implants conformably filled the medullary canal, while active cortical bone remodeling and apposition of new periosteal and/or endosteal bone was observed with no significant macroscopic or microscopic observations. Fractured sheep tibiae exhibited increased bone formation inside the osteotomy gap with no significant difference when fixation was augmented by PBSS implants. Periosteal callus size gradually decreased over time and was similar in both treatment groups. No inhibition of endosteal bone remodeling or vascularization was observed with PBSS implants. Intramedullary application of a light curable PBSS is a biocompatible, feasible method for fracture fixation.

Keywords

Fracture stabilization; light-curable; intramedullary; biocompatibility; polymer

INTRODUCTION

Splints, casts, metal fixator plates, and intramedullary rods stabilize bone fractures and promote healing.[1] These devices balance immobilization sufficiently to ensure alignment,

Send all correspondence to: Brett Zani, PhD, CBSET, Inc., 500 Shire Way, Lexington, MA 02421, bzani@cbset.org.

while not being restrictive to the point of impairing fracture healing.[2] Current intramedullary fixation systems provide longitudinal stabilization with minimal bending forces, but are limited in contact surface area with bone and as a result require additional hardware to achieve rotational stability, thereby resulting in a concentration of load.[3] Application of external fixtures to bone adds to bulk, protrusion, and other complications. Current devices must be inserted in alignment with the canal of the treated bone and are associated with assorted complications including delayed union, device displacement, and nerve impingement.[4–11] However, intramedullary fixation may be an ideal way to stabilize proximal and distal articular extension fractures, especially if fixation systems can be applied percutaneously, avoiding the need for large tissue dissections.[12]

A percutaneous intramedullary photodynamic bone stabilization system (PBSS) has been developed consisting of a non-compliant, polyethylene terephthalate (PET; Dacron) balloon conforming to the patient's unique medullary canal when filled with liquid monomeric material, which is polymerized *in situ* via application of visible (436 nm) light. Intramedullary fixation is established with extensive longitudinal support and alignment without compromising endosteal remodeling, while negating the need for periosteal dissection or manipulation.[13] Unlike traditional metal hardware, the PBSS may be complimented by pins and screws and/or plates anywhere along the implant to optimize fracture repair as needed for each patient. While the PBSS has been successfully used to stabilize fractures in low-load bearing bones[13], it may provide fracture stabilization in bones bearing greater weight such as the long bones of the leg. We evaluated the biocompatibility and feasibility of this light curable, percutaneous intramedullary balloon stabilization system within sheep tibiae in the presence and absence of fracture.

MATERIALS AND METHODS

Non-fracture model

Unilateral PBSS tibia implantations in 18 skeletally mature, Polypay sheep (1–4 years old, 60–98 kg) were conducted under an approved Institutional Animal Care and Use Committee (IACUC) protocol at CBSET, Inc. in Lexington, MA. Following intravenous anesthesia, intubation, and maintenance with isoflurane, under aseptic conditions the anterior edge of the left tibial plateau was exposed and a small entry portal made into the oblique area using a surgical awl. Sequential drilling into the medullary canal was performed with 3–5 mm and then 8 mm drill bits with a guide wire advanced for assistance in maintaining correct orientation and angle. Drilling ended at the transit point of trabecular bone to the canal. Medullary canal contents (eg, adipose, hematopoietic elements, "marrow") were aspirated, the canal cleaned with a cylindrical stainless steel wire brush and lavaged/aspirated repeatedly with sterile saline. The PBSS (11 × 160 mm) was inserted into the intramedullary canal under fluoroscopic guidance and then filled with liquid monomer. The light source (436 nm) was then activated for 800 seconds to cure the monomer into polymer. The catheter was separated from the implant leaving the polymer-filled implant in the medullary canal. The surgical incision was closed and the animals recovered. Animals were euthanized at 30, 90, and 180 days postoperatively (n=6 at each time point, Table I).

Treated and contralateral untreated tibiae were harvested, cleaned of soft tissue and immersed in 10% neutral-buffered formalin (NBF). The joint capsule of treated tibiae were also collected in NBF and processed. High-resolution radiographs (Faxitron X-Ray Corporation®) were obtained of all fixed, treated tibiae and one contralateral/untreated tibia from each time point in two orthogonal planes prior to processing/trimming. The treated and untreated tibiae, joint capsules (treated sites), lungs, and any macroscopic observations from examining the external body surface, all orifices, cranial, thoracic, abdominal cavities and their contents were processed and stained with hematoxylin and eosin (H&E). Undemineralized, treated tibiae and one untreated tibia from each time point were sawed in five equally spaced cross-sections from the diaphysis of all tibiae as well as one cross section through each metaphysis. Each section was resin embedded (methylmethacrylate), ground, polished and H&E stained to define repair, including inflammation, necrosis, hemorrhage, and adverse events. Histopathologic parameters were graded by a pathologist blinded to each sample as follows: 0 = absent; 1 = minimal/unremarkable; 2 = mild to moderate; 3 = marked/severe. The percentage of medullary canal filled by PBSS was graded as follows: 1 = <25%; 2 = 25%–75%; 3 = >75%. Apposition of PBSS to the endosteal surface of the medullary canal was assessed as follows: 0 = no apposition; 1 = < 25%; 2 = 25%–75%; 3 = >75% apposition.

Fracture model

Tibia fracture studies were conducted under an approved animal use protocol at the AO Foundation in Davos, Switzerland. Forty skeletally mature (2–4 years old, similar weight and size) Swiss Alpine sheep with medullary canals of at least 8 mm were anesthetized and maintained with isoflurane. Under aseptic conditions, a medial para-patellar right femoro-tibial arthrotomy was performed in all animals to provide access to the proximal aspect of the right tibial crest, which was drilled and accessed with a guide wire. The medullary canal was accessed using cannulated 4 mm drill bits followed by 6 mm diameter drill bits. The opening was enlarged with an 8.5 mm diameter hand reamer. A 1.5 mm guide-wire was introduced in the canal and correct placement verified by fluoroscopy. The medullary canal contents were aspirated, the canal cleaned with a cylindrical stainless steel wire brush and lavaged/aspirated repeatedly with sterile lactated Ringer's solution. The most proximal and distal fixator screws, 4 mm Schanz screws, were first inserted allowing for an 11 mm diameter, 200 mm long stainless steel connecting bar to be applied between the screws using 2-part connecting bolts. Holes were drilled in the cis-cortex using the connecting bars and bolts as drill guides for the 2 remaining 4 mm Schanz screws. The drill bits were left in place for stabilization during the osteotomy.

Each animal received a short oblique mid-diaphysis right tibia osteotomy using an oscillating saw and was then randomly assigned to one of the following experimental groups (Table 1): (1) stabilization with a 3/3 type Ia external fixator and double connecting bar (8 weeks, n=6); (2) stabilization with a 2/2 type Ia external fixator, double connecting bar and 13 × 160 mm PBSS (8 weeks, n=6); (3) stabilization with a 3/3 type Ia external fixator and double connecting bar (12 weeks, n=8); (4) stabilization with a 2/2 type Ia external fixator, double connecting bar and 13 × 160 mm PBSS (12 weeks, n=8); (5) stabilization with a 2/2 type Ia external fixator, double connecting bar and 13 × 160 mm PBSS (26 weeks, n=8).

In Groups 1 and 3 (non-PBSS treated groups), the osteotomy was reduced, and the remaining fixator screws applied and bolted to the connecting bar. For Groups 2, 4, and 5 (PBSS treated groups), the osteotomy was reduced and the PBSS deployed across the osteotomy. Sufficient liquid monomer was then infused to fully inflate the balloon. The monomer was then cured by visible light activation (436 nm). Drilling of the 2 holes in the cis-cortex was completed through the cured polymer and the trans-cortex. The remaining fixator screws were then applied followed by surgical incision site closure and limb bandaging.

Sheep were recovered in a harness for 8 weeks to allow full weight bearing, but limiting motion to prevent the sheep from lying down. The harness was reset and changed on a regular basis. In Group 5, 1 connecting bar of the external fixator was removed 16 weeks after the surgery and 3 weeks later all pins were removed under sedation. The animals were maintained in a harness for 1 week and received antibiotics for 3 days after removal of the pins.

Standard antero-posterior radiographs of the tibial surgical sites were obtained immediately post-operatively and biweekly until euthanasia in all animals. The radiographs were used to monitor for signs of bone infection, remodeling, and pin loosening. Animals were euthanized at 8, 12 or 26 weeks. Tibiae were collected and fixed in 70% ethanol for 4 weeks. During fixation, high resolution radiographs (Faxitron X-Ray Corporation®) were obtained. Fixed samples were scanned using 3D peripheral quantitative computed tomography (XtremeCT, SCANCO Medical, Brüttisellen, Switzerland) with an isotropic resolution of 82 μm. The scanned region was confined to the transfixation pins located immediately proximal and immediately distal to the osteotomy site. After reconstruction, the 3D data were reoriented to place the osteotomy in a planar view. Callus volume and callus density were determined from voxel count and average voxel density in the images, respectively. New bone formation was assessed within a region of interest (ROI) drawn on the osteotomy. New bone volume and density were then assessed within the ROI.

Following fixation, samples were embedded in polymethyl methacrylate (PMMA) and trimmed into 3 blocks per tibia. One block included the osteotomy site (OS) and two selected fixator screw/PBSS interface sites (Figure 1). Sections were glued with cyanoacrylate onto opaque Plexiglas slides, ground and polished to a final thickness of 85–145 μm and stained with Giemsa/Eosin. Popliteal lymph nodes were fixed in 4% NBF for 2 weeks, processed and stained with H&E. Qualitative and semi-quantitative histopathological analyses by a pathologist blinded to each sample was performed via light microscopy (Axioplan, Zeiss®) and graded as: 1 = minimal/unremarkable/very few /very small; 2 = slight/few /small; 3 = moderate/moderate number/moderate size; 4 = marked/many/large; 5 = massive/very large number/very large size. The relative amount of bone tissue at the osteotomy site was determined by defining several ROIs directly inside the osteotomy gap (not including the medullary area) and placing the ROIs manually over digitized radiographs. Bone tissue in the non-implant area was assessed by threshold setting with the aid of histomorphometric software (Axiovision, Zeiss®) and a custom made macro (KS400, Zeiss®). The relative amount of bone (in % bone / ROI) was calculated for each animal and averaged by treatment group.

Statistical analysis

Statistical evaluation was performed using SPSS for Windows (version 18.0). MicroCT analysis of callus volume and density, and new bone volume and density were evaluated for normality distribution (using a Shapiro-Wilk test) and univariate ANOVA followed by Bonferonni post hoc test to detect significance differences between treatment groups. For all statistical tests, a p-value ≤ 0.05 was considered significant. Summary of data for histologic parameters (including but not limited to inflammation, necrosis, hemorrhage, etc.) are presented as scoring results per recovery interval in a descriptive statistics format (mean and standard deviation scores) to allow qualitative comparisons between groups; without statistical analysis.

RESULTS

Non-fracture model

All treated sheep survived to study endpoints. No macroscopic indications of adverse systemic effects were observed in any animal at 30, 90 or 180 days. There were variable increases in the radiographic opacity of the treated tibiae relative to the untreated controls within each time point, most likely due to the reactive bone apposition response to the PBSS (Figure 2). The PBSS filled and conformed to the diaphyseal medullary canal and was apposed (>75% apposition) to the diaphyseal cortical bone with only minimal/unremarkable loss of apposition in the most proximal plane due to widening of the medullary canal (Table 2). Progressive, but minimal/unremarkable, ossification was observed by Day 180; balloon-associated inflammation and fibrosis were minimal/unremarkable at all time points (Table 2).

No significant microscopic observations (eg, necrosis, exuberant inflammation, fibrosis) were associated with the joint capsule of treated tibiae or lungs. Cortical bone apposition was primarily periosteal at 30 and 90 days. Endosteal apposition of new bone was minimal to mild at all time points and typically associated with medullary trabecular bone formation. Bone marrow elements were absent from the diaphyseal medullary canal of treated tibiae (Figure 3). Cortical bone necrosis was variable, but generally mild to moderate at 30, 90 and 180 days; mild to moderate remodeling was observed at all time points (Table 3).

Fracture model

Two sheep were euthanized due to surgical difficulties encountered during the initial phases of the study and three sheep were euthanized due to failure of stabilization either associated with the initial reduction and alignment of the fracture, operative failure to engage the Schanz screw in the trans-cortex, or the failure/breakage of the external fixation system. All received PBSS. The remaining 35 animals reached the predefined study end points. In 3 animals, discontinuities of the PBSS were observed, resulting from post-operative breakage of the completely cured polymer and/or by incomplete intra-operative curing of the monomer. In all cases there was sufficient stability provided by the remaining construct for the osteotomy to heal; however, these animals were excluded from analysis.

Morphometric analysis demonstrated continuously increasing cortical bone formation inside the osteotomy gap up to nearly complete closure at 26 weeks (Table 4 and Figure 4). Micro-CT analysis showed no significant changes in callus volume in both the control and PBSS-treated osteotomy groups between 8 and 12 weeks and declined in the PBSS-treated group by 26 weeks (Figure 5A). Conversely callus density significantly increased in both groups between 8 and 12 weeks and significantly increased further in the PBSS group at 26 weeks (Figure 5B). Bone volume within the osteotomy was similar in both groups and remained constant over time (Figure 6A), while bone density was similar for both treatments at 8 and 12 weeks and significantly increased in the PBSS group at 26 weeks (Figure 6B). Statistical analysis indicated no significant difference between the performance of the control and PBSS groups within a given time point.

Osteointegration of the fixator screws proximal and distal to the osteotomy site was mild to moderate, characterized by large bone/implant contact, at 8 and 12 weeks for both groups (Table 5). At 26 weeks in the PBSS group, where the fixator screws were already removed, closure of the screw holes was already moderate and characterized by bony in-growth, suggesting that healing was not affected by the polymerized material. Minimal/unremarkable histiocytic inflammation, characterized by formation and clustering of foamy macrophages was observed locally at the implantation site in some PBSS-treated animals, while clusters of foamy macrophages were observed in local popliteal lymph nodes both in untreated and PBSS-treated animals.

Additionally, the periosteal callus size gradually decreased over time and was similar for both treatment groups. The endosteal surface of the cortical bone and the implants were in most cases tightly apposed to each other; however, flat, non-trabecular endosteal bone formation was observed suggesting the PBSS does not inhibit endosteal bone remodeling and/or vascularization.

DISCUSSION

These studies were conducted to gain an understanding for the feasibility of deployment, along with local and systemic biocompatibility of an intramedullary PBSS in high load-bearing bones, such as the tibia. Prior clinical studies have demonstrated utility of this device in low load-bearing bones, such as phalanges, metacarpal, distal radius, radius, ulna, olecranon, clavicle, and fibula.[13] Thus the present study deployed the PBSS in long bones to examine the resulting local tissue and healing response in the presence or absence of fracture.

The PBSS is a percutaneously delivered balloon, which conforms to the unique shape of an intramedullary canal when filled with monomer, then cured with visible light to form a hardened polymeric implant. The monomer is a proprietary, multifunctional methacrylate containing several biocompatible monomers and multiple photo initiators that form a thermoset material, which during the curing process becomes a cross-linked polymer that retains strength and shape, while being well suited for long-term, permanent devices. Confirmation of polymerization *in vivo* can be performed via MRI scanning of the treated bone. The liquid, uncured monomer displays as white, while the cured polymer displays as

black on an MRI scan. If the material does not cure after exposure to visible light, then the monomer can be exposed to visible light again or aspirated out through the catheter and replaced.

During the curing process, the exothermic response of the material remains relatively low with *in vitro* core temperatures of ~62 °C. Core temperatures of polymethyl methacrylate (PMMA), a bone cement frequently used for clinical applications in orthopedic surgery, have been measured *in vitro* at ~77 °C.[14,15] The thermal excursion for both materials *in vivo* are likely to be substantially reduced in bone due to the mass of the surrounding body, presence of blood flow and thermal conduction and dissipation.

In the non-fracture model, the presence of the PBSS did not preclude bone repair as evidenced by periosteal and/or endosteal apposition of new bone and active, progressive remodeling of the necrotic cortical bone. Healing progressed throughout the study with the PBSS. Variable necrosis of the tibial diaphyseal cortical bone is consistent with the cortical necrosis reported as a common sequela to the surgical manipulation of the medullary canal of long bones (i.e., fracture repair). Such reaction is related to the physical disruption of the endosteum and its blood supply associated with canal clearing (irrigation/aspiration and abrasion by brushing).[16–18] Regardless, physiologic remodeling of the treated tibial cortex was still attained with the PBSS even with the initial cortical necrosis, and the limited re-establishment of the endosteum due to the intimate apposition of the balloon to the cortical endosteal surface. Ancillary external stabilization was determined to be necessary in the fracture model as the canal size in sheep tibiae is small, and static loads experienced by sheep tibiae are greater than those the implant can resist. This is especially the case in bending and deformation, especially as most of the tibia was subjected to greater bending loads than axial loading. The mean cortical bone formation inside the osteotomy gap was 50–60% at 8 weeks postoperatively and increased to 70–80% at 26 weeks. The mean relative bone area was slightly higher in the PBSS-treated animals compared to controls. New bone volumes were similar in PBSS-treated and untreated groups. Callus volumes decreased, while callus densities and new bone densities increased in the PBSS-treated group over time. Also, even with tight apposition of the PBSS and the endosteal surface of cortical bone, flat, non-trabecular endosteal bone formation was observed. Thus in the fracture model, as in the non-fracture model, the PBSS did not appear to prevent new bone formation.

With potential extramedullary embolization from manipulation of the intramedullary canal, the impact of this new device was also examined in peripheral tissues, specifically, the lung and popliteal lymph nodes. Pulmonary inflammation and infarction is a potential adverse response associated with the surgical manipulation of long bones, primarily associated with the embolization of adipose tissue or liquefied fat, secondary to the increased intramedullary pressure, during disruption of bone marrow necessary for the implantation of intramedullary fixation devices.[19–21] The rare embolization of liquid phase bone resins (e.g., PMMA) to the lungs has been reported.[22,23] However, there was no evidence of pulmonary embolization in PBSS non-fracture sheep associated with long bone surgical treatment. In the sheep fracture model, parafollicular clusters of foamy macrophages were observed in the ipsilateral

draining popliteal lymph nodes with a comparable incidence and intensity in both PBSS and untreated groups and thus may not be related to the PBSS.

Intramedullary fixation offers conformable stabilization in the main plane of fracture alignment and force. Use of a light curable polymer-filled balloon can achieve such fixation in a personalized manner and with minimal adverse effects - similar to those seen with currently used devices for fracture stabilization. Intramedullary application of a light curable PBSS is a feasible and biocompatible method for fracture fixation in load-bearing bones.

ACKNOWLEDGEMENTS

The authors thank Amanda Botta and Rami Tzafriri for reviewing the manuscript. Robert Rabiner is President and a member of the board of directors for IlluminOss Medical, Inc. This study was supported in part by National Institutes of Health grant (R01 GM-49039) to Dr. Edelman.

REFERENCES

1. Perren SM. Physical and biological aspects of fracture healing with special reference to internal fixation. Clin Orthop Relat Res. 1979; (138):175–196. [PubMed: 376198]
2. Chao EY, Inoue N, Elias JJ, Aro H. Enhancement of fracture healing by mechanical and surgical intervention. Clin Orthop Relat Res. 1998; (355 Suppl):S163–S178. [PubMed: 9917637]
3. Bucholz, RWHJ.; Court-Brown, CM.; Tornetta, P.; McQueen, MM.; Ricci, WM. Rockwood and Green's Fractures in Adults. Vol. 1. Pennsylvania: Lippincott Williams & Wilkins; 2010.
4. Singisetti K, Ambedkar M. Nailing versus plating in humerus shaft fractures: a prospective comparative study. Int Orthop. 2009; 34(4):571–576. [PubMed: 19506868]
5. Changulani M, Jain UK, Keswani T. Comparison of the use of the humerus intramedullary nail and dynamic compression plate for the management of diaphyseal fractures of the humerus. A randomised controlled study. Int Orthop. 2007; 31(3):391–395. [PubMed: 16900354]
6. Koike Y, Komatsuda T, Sato K. Internal fixation of proximal humeral fractures with a Polarus humeral nail. J Orthop Traumatol. 2008; 9(3):135–139. [PubMed: 19384609]
7. McCormack RG, Brien D, Buckley RE, McKee MD, Powell J, Schemitsch EH. Fixation of fractures of the shaft of the humerus by dynamic compression plate or intramedullary nail. A prospective, randomised trial. J Bone Joint Surg Br. 2000; 82(3):336–339. [PubMed: 10813165]
8. Taljanovic MS, Jones MD, Ruth JT, Benjamin JB, Sheppard JE, Hunter TB. Fracture fixation. Radiographics. 2003; 23(6):1569–1590. [PubMed: 14615566]
9. Miller NC, Askew AE. Tibia fractures. An overview of evaluation and treatment. Orthop Nurs. 2007; 26(4):216–223. quiz 224-5. [PubMed: 17882096]
10. Strecker W, Suger G, Kinzl L. Local complications of intramedullary nailing. Orthopade. 1996; 25(3):274–291. [PubMed: 8766665]
11. Bostman O, Varjonen L, Vainionpaa S, Majola A, Rokkanen P. Incidence of local complications after intramedullary nailing and after plate fixation of femoral shaft fractures. J Trauma. 1989; 29(5):639–645. [PubMed: 2724381]
12. Fuchtmeier B, Brockner S, Hente R, Maghsudi M, Nerlich M, Prantl L. The treatment of dislocated humeral head fractures with a new proximal intramedullary nail system. Int Orthop. 2008; 32(6): 759–765. [PubMed: 17598111]
13. Heck, S.; Gicki, S.; Rabiner, B.; Penne, D. Initial clinical experiences with a photodynamic polymer (IlluminOss); Med Review: Journal for Medical Continuing Education Conferences (German); 2012. p. 15-16.
14. Kuehn KD, Ege W, Gopp U. Acrylic bone cements: composition and properties. Orthop Clin North Am. 2005; 36(1):17–28. v. [PubMed: 15542119]
15. Lai PL, Chen LH, Chen WJ, Chu IM. Chemical and physical properties of bone cement for vertebroplasty. Biomed J. 2013; 36(4):162–167. [PubMed: 23989310]

16. Brumback RJ, Virkus WW. Intramedullary nailing of the femur: reamed versus nonreamed. J Am Acad Orthop Surg. 2000; 8(2):83–90. [PubMed: 10799093]
17. Pape HC, Giannoudis P. The biological and physiological effects of intramedullary reaming. J Bone Joint Surg Br. 2007; 89(11):1421–1426. [PubMed: 17998175]
18. Leunig M, Hertel R. Thermal necrosis after tibial reaming for intramedullary nail fixation. A report of three cases. J Bone Joint Surg Br. 1996; 78(4):584–587. [PubMed: 8682825]
19. Schult M, Frerichmann U, Schiedel F, Brug E, Joist A. Pathophysiology of fat embolism after intramedullary reaming. Eur. J. Trauma. 2003; 29:68–73.
20. Lindwer J, Van Den Hooff A. The influence of acrylic cement on the femur of the dog. A histological study. Acta Orthop Scand. 1975; 46(4):657–671. [PubMed: 1180027]
21. Padovani B, Kasriel O, Brunner P, Peretti-Viton P. Pulmonary embolism caused by acrylic cement: a rare complication of percutaneous vertebroplasty. AJNR Am J Neuroradiol. 1999; 20(3):375–377. [PubMed: 10219399]
22. Tozzi P, Abdelmoumene Y, Corno AF, Gersbach PA, Hoogewoud HM, von Segesser LK. Management of pulmonary embolism during acrylic vertebroplasty. Ann Thorac Surg. 2002; 74(5):1706–1708. [PubMed: 12440642]
23. Yoo KY, Jeong SW, Yoon W, Lee J. Acute respiratory distress syndrome associated with pulmonary cement embolism following percutaneous vertebroplasty with polymethylmethacrylate. Spine (Phila Pa 1976). 2004; 29(14):E294–E297. [PubMed: 15247590]

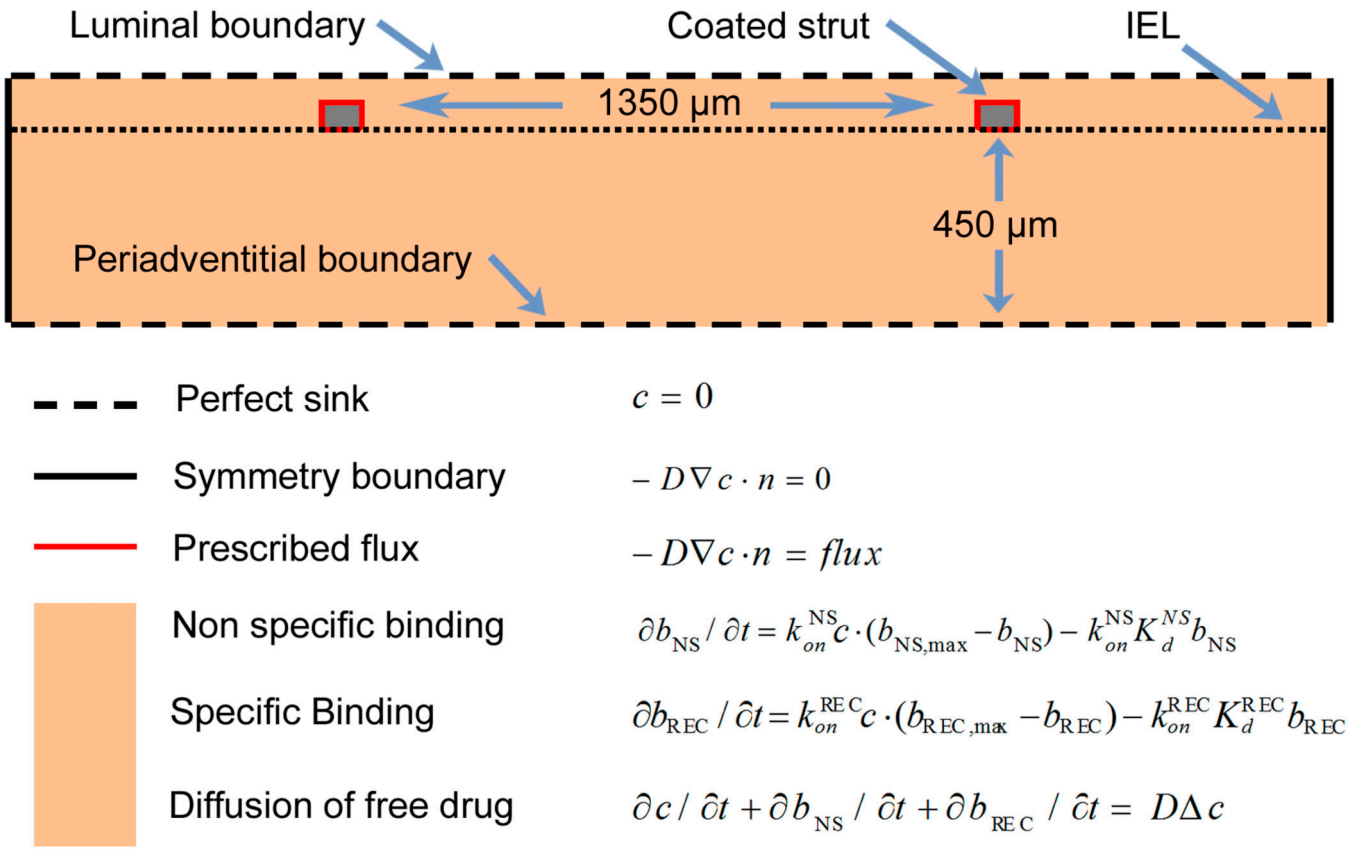

Figure 1.
Trimming scheme in fracture model depicting location and size of the 3 blocks in which each tibia was trimmed (A: control without PBSS; B: test with PBSS). OS: osteotomy site. P2/3/5: designate Shanz screw sites.

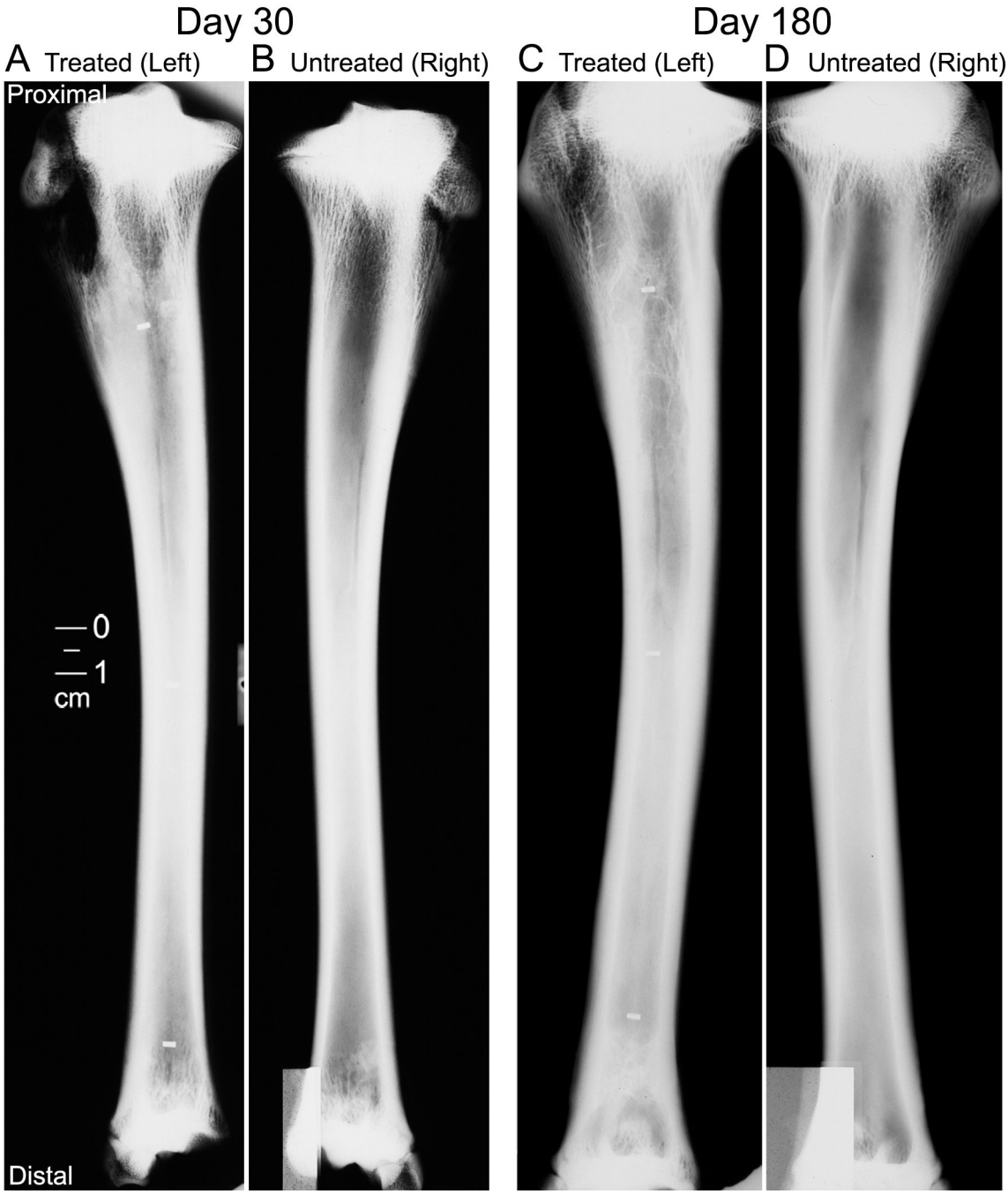

Figure 2.
High resolution x-rays of sheep tibiae 30 days (A & B) and 180 days (C & D) in non-fracture model following treatment with either a PBSS or no treatment. All views medial-lateral.

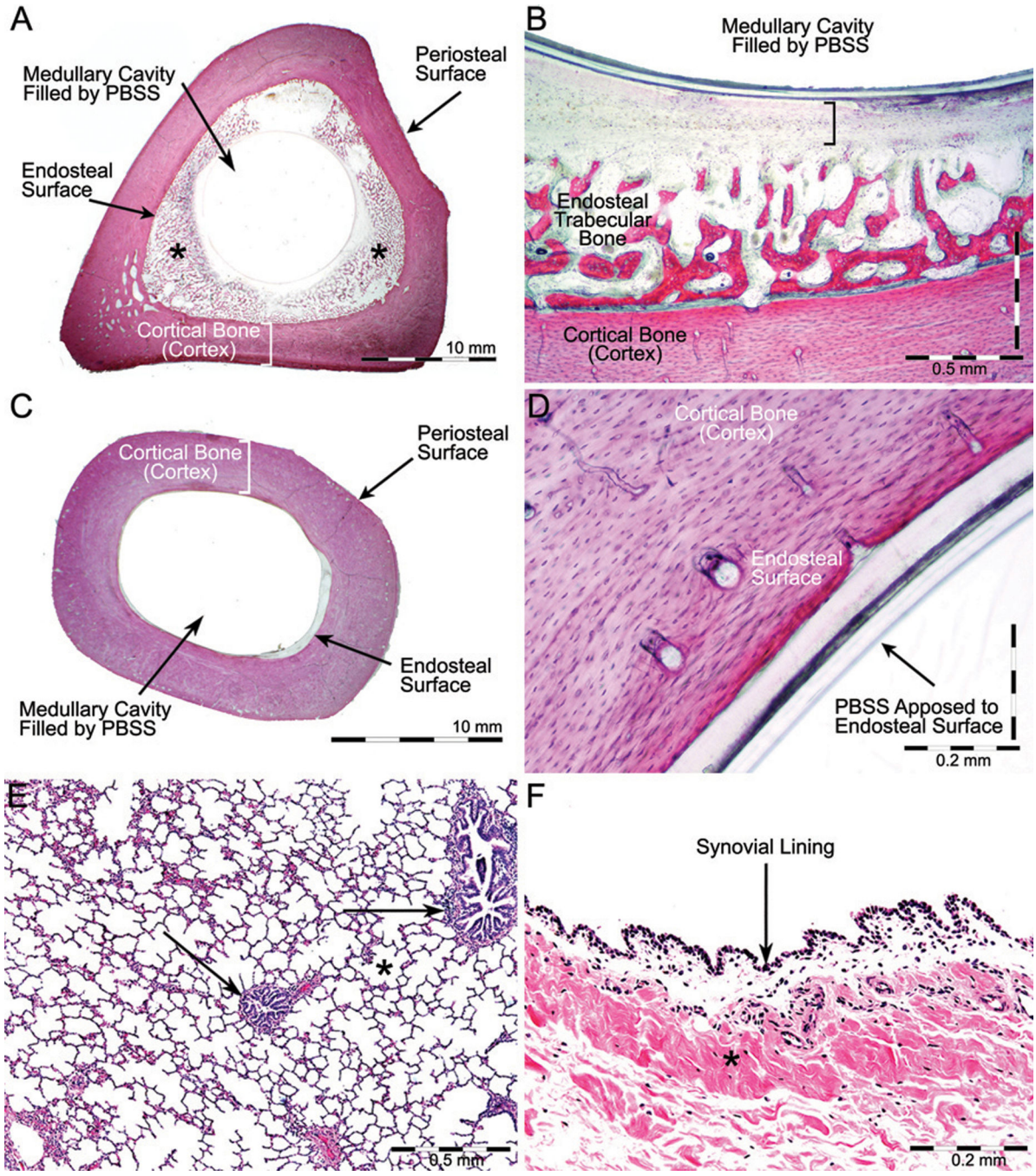

Figure 3.

Examples of metaphyseal (A & B) and diaphyseal (C & D) sheep tibiae 30 days post-treatment in non-fracture model. (A) Peri-balloon trabecular bone formation is designated by asterisks. (B) Mild peri-balloon fibrosis (bracket) and trabecular bone formation displayed in metaphyseal tibia. (C) Medullary cavity filled by PBSS in diaphyseal tibia. (D) PBSS is completely apposed to the endosteal surface of the cortex. No evidence of adverse changes were associated with (E) lungs - note open alveolar spaces (asterisk) and bronchioles

(arrows) – and (F) joint capsules of tibiae - note inner lining of joint capsule (asterisk) covered by normal synovial lining (arrow) - from PBSS-treated animals.

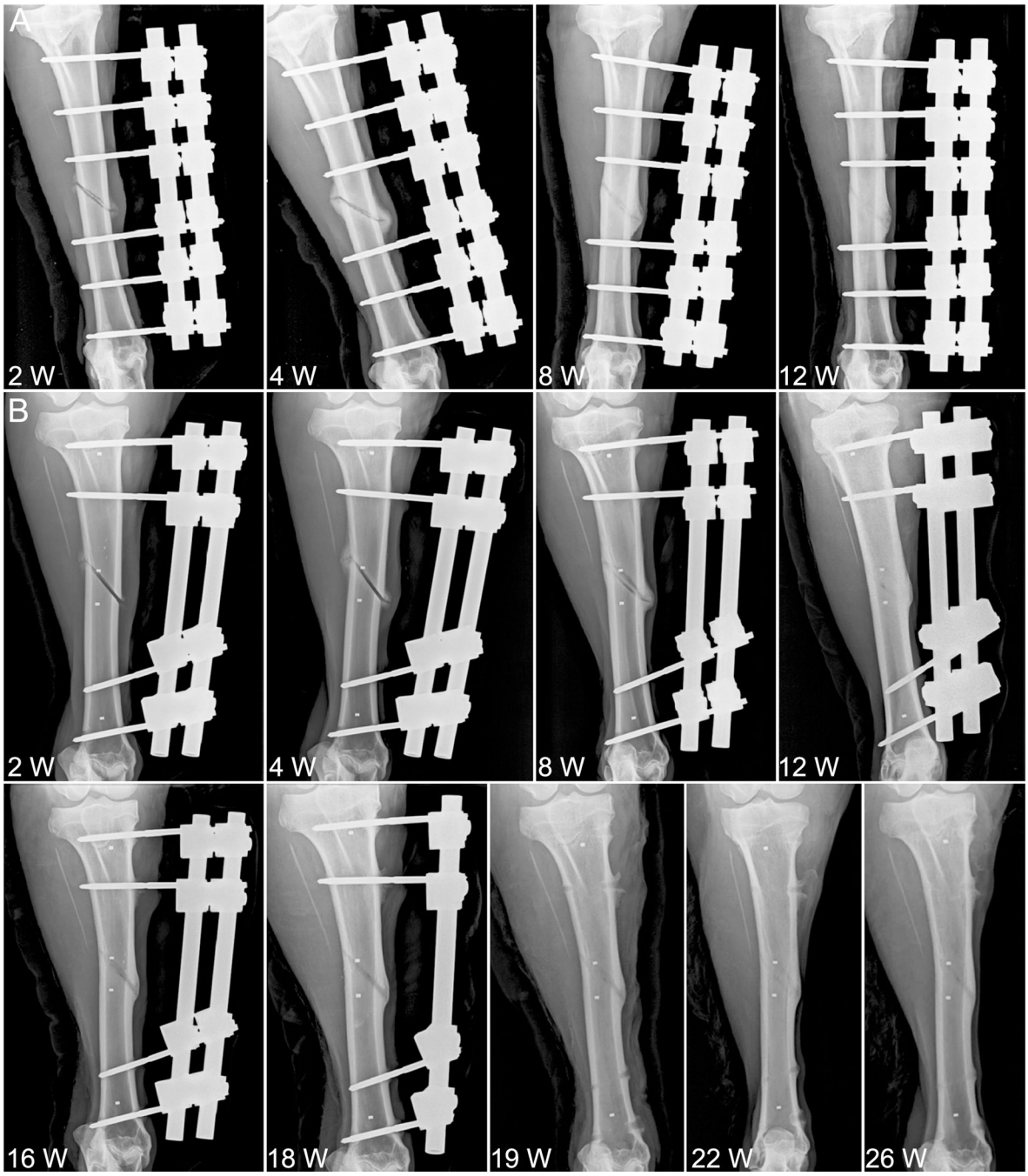

Figure 4.

Radiographs of the fracture model with (A) a sheep tibia stabilized with a 3/3 type Ia external fixator and double connecting bar (Group 3) up to 12 weeks; (B) PBSS-treated animal (Group 5) with a 2/2 type Ia external fixator and double connecting bar showing continuously increasing cortical bone formation inside the osteotomy gap up to nearly complete closure at 26 weeks. External fixator was removed after 19 weeks.

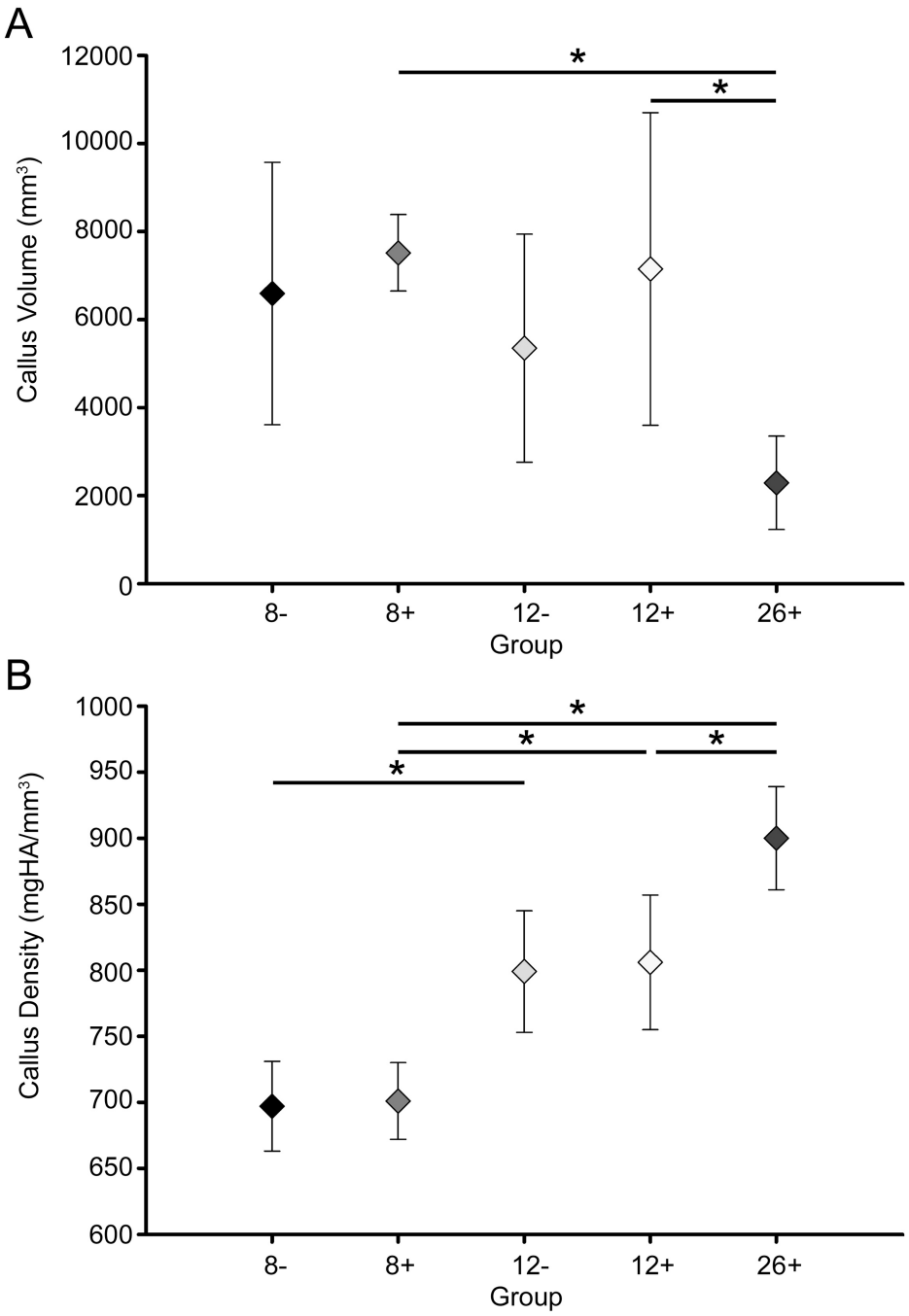

Figure 5.

Callus volume (A) and density (B) in fracture model, as determined by μCT. Fractured sheep tibiae were stabilized with a 3/3 type Ia external fixator and double connecting bar (−) or a 2/2 type Ia external fixator, double connecting bar, and 13 × 160 mm intramedullary PBSS (+). Values are mean±sd; * denotes statistically significant group differences.

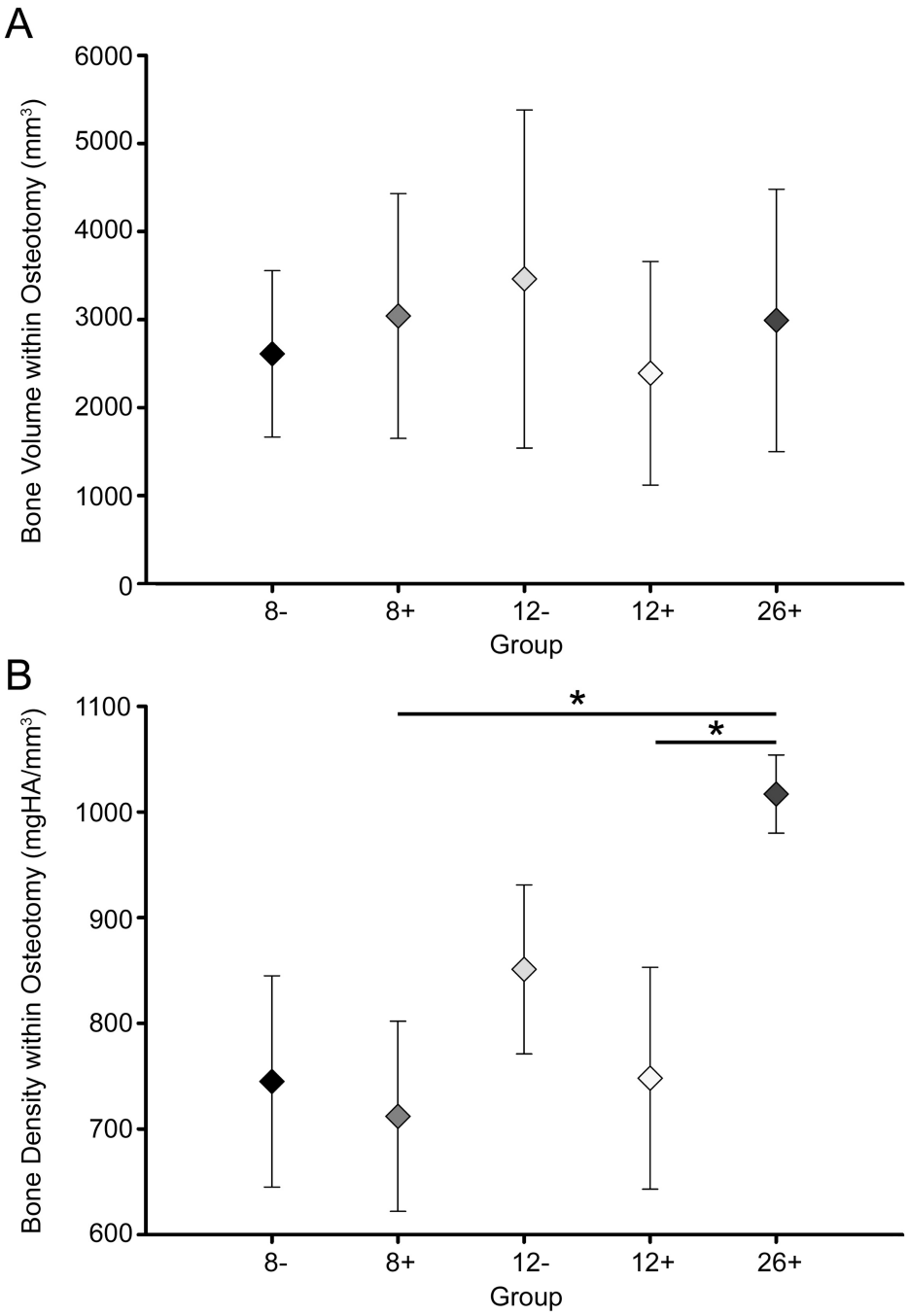

Figure 6.

New bone volume (A) and density (B) within the osteotomy in fracture model, as determined by microCT. Fractured sheep tibiae were stabilized with a 3/3 type Ia external fixator and double connecting bar (−) or a 2/2 type Ia external fixator, double connecting bar, and 13 × 160 mm intramedullary PBSS (+). Values are mean ± sd; * denotes statistically significant group differences).

TABLE I

Sheep Tibiae Implant Matrix

Tibia Model	Time Point	PBSS Implant	External Fixator	n=
Non-Fracture				
Group 1	30 Days	11 × 160 mm	-	6
Group 2	90 Days	11 × 160 mm	-	6
Group 3	180 Days	11 × 160 mm	-	6
Fracture				
Group 1	8 Weeks	-	3/3 Ia	6
Group 2	8 Weeks	13 × 160 mm	2/2 Ia	3
Group 3	12 Weeks	-	3/3 Ia	8
Group 4	12 Weeks	13 × 160 mm	2/2 Ia	7
Group 5	26 Weeks	13 × 160 mm	2/2 Ia	8

TABLE II

Tissue Response to PBSS of Sheep Tibiae in Non-Fracture Model*

	30 Days (n=6)	90 Days (n=6)	180 Days (n=6)
Peri-Balloon Fibrosis	0.45 ± 0.69 34%	0.53 ± 0.57 50%	0.43 ± 0.50 43%
Peri-Balloon Inflammation	0.45 ± 0.74 34%	0.57 ± 0.50 57%	0.60 ± 0.50 60%
Peri-Balloon Ossification	0.00 ± 0.00 0%	0.10 ± 0.31 10%	0.27 ± 0.45 27%
Balloon Diaphyseal Medullary Cavity Filling	3.00 ± 0.00 100%	3.00 ± 0.00 100%	3.00 ± 0.00 100%
Balloon Diaphyseal Cortex Apposition	2.21 ± 1.18 83%	2.50 ± 1.01 90%	2.38 ± 1.12 86%

* Values are mean and standard deviation of scores (0–3) and frequency [%] of observations.

TABLE III

Bone Response to PBSS of Sheep Tibiae in Non-Fracture Model*

	30 Days (n=6)	90 Days (n=6)	180 Days (n=6)
Cortical Bone Necrosis	1.52 ± 0.57 100%	2.43 ± 0.57 100%	1.77 ± 0.43 100%
Endosteal Cortical Bone	0.52 ± 0.51 52%	1.37 ± 0.72 97%	1.20 ± 0.71 83%
Periosteal Cortical Bone	1.34 ± 0.55 100%	2.07 ± 0.83 100%	1.40 ± 0.72 90%
Medullary Trabecular Bone	0.28 ± 0.53 24%	0.77 ± 0.94 50%	1.10 ± 0.66 83%
Active Cortical Bone Remodeling	1.72 ± 0.53 100%	2.23 ± 0.57 100%	1.77 ± 0.50 100%

* Values are mean and standard deviation of scores (0–3) and frequency [%] of observations.

TABLE IV

Relative Bone Area in the Osteotomy Gap of Fracture Model*

	Group 1 (n=6)	Group 2 (n=3)	Group 3 (n=8)	Group 4 (n=7)	Group 5 (n=8)
Bone Area	48.82 ± 11.39	62.46 ± 4.10	65.17 ± 7.65	66.82 ± 7.45	79.98 ± 7.72
Postoperative Weeks	8	8	12	12	26

*The values are given as the mean percentage and standard deviation.

TABLE V

Osteointegration of Fixator Screws in Fracture Model*

	Group 1 (n=6)	Group 2 (n=3)	Group 3 (n=8)	Group 4 (n=7)	Group 5 (n=8)
Proximal to Osteotomy					
Grade	4.33 ± 0.52	4.00 ± 1.00	4.25 ± 0.71	3.29 ± 0.95	3.25 ± 0.46
Distal to Osteotomy					
Grade	4.17 ± 0.75	4.00 ± 0.58	4.00 ± 0.76	3.43 ± 0.53	3.00 ± 0.52
Incidence	6	3	8	7	8
Postoperative Weeks	8	8	12	12	26

* The values are given as the mean grade (1–5) and standard deviation and incidence (crosses) of osteointegration. Group 5 was 7 weeks post-fixator screw removal.